Modeling arsenic deactivation through arsenic-vacancy clusters using an atomistic kinetic Monte Carlo approach

R. Pinacho,[a] M. Jaraiz, P. Castrillo, I. Martin-Bragado, J. E. Rubio, and J. Barbolla
Department of Electronics, University of Valladolid, 47011 Valladolid, Spain

(Received 29 November 2004; accepted 10 May 2005; published online 13 June 2005)

A comprehensive atomistic model for arsenic in silicon which includes charge effects and is consistent with first-principles calculations for arsenic-vacancy cluster energies has been developed. Emphasis has been put in reproducing the electrical deactivation and the annealed profiles in preamorphized silicon. The simulations performed with an atomistic kinetic Monte Carlo simulator suggest a predominant role of the mobile interstitial arsenic in deactivation experiments and provide a good understanding of the arsenic behavior in preamorphized silicon during annealing. © *2005 American Institute of Physics*. [DOI: 10.1063/1.1948533]

Due to the continuous shrinkage of device dimensions, superficial silicon layers doped with ever higher arsenic (As) concentrations are required in current semiconductor technology. These layers present a higher electrical resistance than expected,[1] attributed to the As clustering phenomena . More specifically, many theoretical studies[3–5] in addition to recent experiments[6,7] have proven the high stability of electrically inactive As clusters formed by a vacancy (V) surrounded by substitutional As atoms (As_nV), with $n=2$, 3, 4.

In this work, we present a comprehensive atomistic model for As in Si that, with a reduced set of As_nV_m cluster parameters, can account for As electrical deactivation and reproduce the As behavior in preamorphized As implantations while being also consistent with first-principles calculations for the As_nV_m cluster energetics. In order to test the model, simulations were performed with the atomistic kinetic Monte Carlo simulator DADOS[8] which allows to incorporate the new As model to the previously implemented models for the rest of the Si phenomena taking place during annealing, such as amorphous layer,[9] end-of range {311},[10] and dislocation loops generation/dissolution and As segregation sweep during solid phase epitaxial regrowth (SPER), without the penalty of an increased computation time.

Arsenic diffusion is assisted via both, vacancy and interstitialcy mechanisms.[11] In order to reproduce it, the model includes two atomistic mobile configurations, arsenic-vacancy pair (AsV) and interstitial arsenic (As_i), while the substitutional As (As_s) was considered immobile and electrically active. The reactions that control As diffusion are then:

$$As_s + V \leftrightarrow AsV, \tag{1a}$$

$$As_s + I \leftrightarrow As_i, \tag{1b}$$

$$AsV + I \leftrightarrow As_s, \tag{1c}$$

$$As_i + V \leftrightarrow As_s, \tag{1d}$$

where V and I stand for mobile vacancies and self-interstitials, respectively.

Moreover, high As concentrations demand a correct description of extrinsic diffusion. This and other Fermi level related effects have been recently included in DADOS and a detailed description of the physical modeling can be found in a recent publication.[12] Table I summarizes the energetics of the mobile species involved in As diffusion. The migration and binding energies of AsV^0 are consistent with first-principles calculations[3] while the position of the AsV^- electronic level in the band gap is extracted from well-established deep level transient spectroscopy experiments.[11] Taking into account the high formation energies of V and I, it can be deduced that the reverse reactions of Eqs. (1c) and (1d) require a high energy and consequently do not happen at the usual annealing temperatures. With the values of Table I, the total intrinsic As diffusion results

$$D^*_{As} = D^*_{AsV} + D^*_{Asi} = 14.5 \exp(-4.05/kT)\ \mathrm{cm}^2/\mathrm{s} \tag{2}$$

that is used in the TSuprem-IV simulator.[13] The As diffusion fraction due to interstitials is similar to that measured by Matsumoto.[14] The extrinsic As diffusion properly fits the experiments performed by Fair[15] at different temperatures and concentrations.

On the other hand, in order to reproduce As deactivation, the formation of electrically neutral As_nV_m clusters was included. In Fig. 1 the potential energies of the relevant As clusters are summarized. Note that the most stable clusters are As_3V and As_4V, whose formation energies are even lower than isolate substitutional As $[E_f(As_nV) = E_{pot}(As_nV) + E_f(V) < 0]$ in good agreement with calculations.[4] Taking into account that in the As case there are two mobile species (AsV and As_i), the diffusion-assisted growth/shrinkage of the clusters is described by the following reactions in the forward/reverse direction:

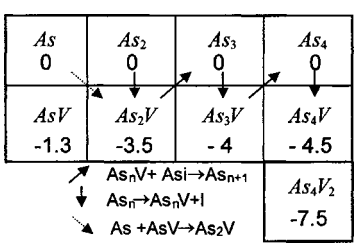

FIG. 1. Potential energy map (in electron-volts) of the As_nV_m clusters. Arrows show the cluster formation path during As deactivation in experiments from Ref. 16 according to our model. The clusters As_nV_m that are not indicated are supposed to be more unstable (high potential energy) so they do not appear in these conditions.

[a]Electronic mail: rutpin@tel.uva.es

$$As_nV_m + V \leftrightarrow As_nV_{m+1} \quad \text{V trapping/emission,} \quad (3)$$

$$As_nV_m + AsV \leftrightarrow As_{n+1}V_{m+1} \quad \text{AsV trapping/emission,} \quad (4)$$

$$As_nV_m + I \leftrightarrow As_nV_{m-1} \quad \text{I trapping/emission,} \quad (5)$$

$$As_nV_m + As_i \leftrightarrow As_{n+1}V_{m-1} \quad As_i \text{ trapping/emission.} \quad (6)$$

The reverse reaction of the last two expressions conveys the formation of an I–V pair in the bulk. The generated vacancy remains immobilized in the cluster while the interstitial is emitted alone [Eq. (5)] or combined with an As [Eq. (6)]. As a consequence, in both cases, an anomalous enhanced As diffusion assisted by the bulk-generated As_i happens.

Notice also that for $n=1$ and $m=0$, the As_nV_m cluster is substitutional As (As_s) and, in the same way, for $n=1$ and $m=1$, the cluster is the mobile AsV. Subsequently, Eqs. (3)–(6) convert into point defect reactions. Some of them appear in Eq. (1). For instance, Eq. (1a) can be deduced from Eq. (3) with $As_nV_m=As_s$. The forward reactions of the rest result in the formation of the smallest As_nV_m clusters: $As_s + AsV \leftrightarrow As_2V$, $AsV + V \leftrightarrow AsV_2$, $AsV + AsV \leftrightarrow As_2V_2$, $AsV + As_i \leftrightarrow As_2$. Finally, the reaction $As_s + As_i \leftrightarrow As_2I$ has not been implemented so that the arsenic-interstitial clusters are considered to be unstable.

In order to reproduce As deactivation, the experiments reported by Rousseau *et al.*[16,17] about As deactivation are very useful because in them electrical deactivation is isolated from implant damage kinetics. These experiments reveal that, in the first stages, As deactivation is fast and generates a high concentration of self-interstitials that enhances As diffusion. It is proposed that arsenic deactivation could be produced by the formation of As_nV clusters with the injection of an I into the bulk. These authors also claim that the same process would take place during any As deactivation whether it be previously deactivated and reactivated arsenic[18] or following solid phase regrowth.[19]

In Fig. 2, the experimental structure from Rousseau *et al.*[16] and its DADOS simulation are shown. The structure consists of a buried boron layer as an interstitial detector and a fully activated high concentration (4.5×10^{20} cm^{-3}) As doped laser melt annealed surface layer. Dopant profiles were measured by secondary ion mass spectroscopy (SIMS). Our model is able to reproduce the temporal evolution of the whole process. At the beginning, all the arsenic atoms are electrically active. Therefore, in the simulations, the As atoms are supposed to stay initially in substitutional positions. Assuming a randomized As atoms distribution, for this high As concentration there is a high probability of two, three, or four As atoms to be placed at a small distance in the Si lattice. Taking into account that the potential energy of As_2, As_3, and As_4 clusters is the same as substitutional As (see Fig. 1), during the temperature ramp-up, As_n clusters are generated in the bulk from the substitutional As atoms that are placed closer to each other than the capture (second neighbors) distance. Once the As_2, As_3, and As_4 clusters have appeared, the reverse reaction (5) is energetically more favorable, especially in the case of As_3V and As_4V formation. Therefore, these reactions take place, generating interstitials that diffuse, interact with substitutional As atoms and form As_i. The mobile As_i increase As diffusion and join the already formed As_nV clusters producing their growth, according to the forward (6) and reverse (5) reactions, following the solid arrows shown in Fig. 1. Note that, although the difference between the potential energies of As_nV and As_{n+1} is high, there is no barrier energy for the forward reaction (6). In fact, this reaction implies I–V recombination, being the energy of the process negative ($E=E_{As_{n+1}}-E_{As_nV}+E_{bAs_i}-E_{fI}-E_{fV}$). In Fig. 3 the temporal evolution fo the experimental and simulated deactivated As concentration are plotted. From the simulation, it can be observed that after 2 h annealing, most of the inactive As remains as As_3V and As_4V, being the average number of As surrounding a vacancy 3.4, in good agreement with Lawther *et al.*[7] who found by positron annihilation experiments that the average number of As atoms surrounding a vacancy is >2. It is also important to point out that after approximately 1 min annealing, the concentration of thermally generated vacancies starts to be noticeable and also contribute to the As deactivation in the following way: vacancies join the substitutional As form-

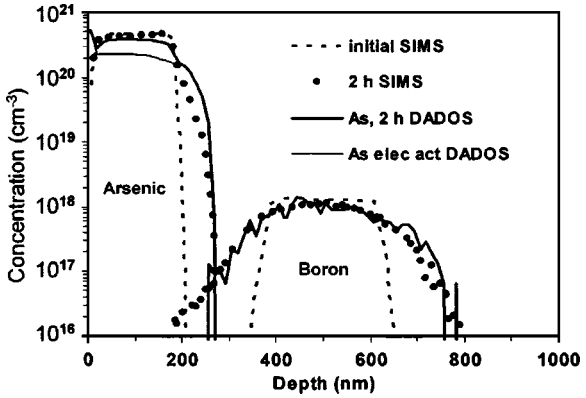

FIG. 2. SIMS data of the structures from Ref. 17 consisting of a buried B layer and an initially fully activated implanted and laser-melt annealed superficial As layer. After 750 °C 2 h annealing, SIMS data show large enhanced diffusion of the buried B layer. DADOS simulation (lines) properly reproduces the As and B profiles.

TABLE I. Atomistic parameters of the species involved in As diffusion. The superscript denotes the charge state of the defect. Diffusivities and concentrations in equilibrium conditions relate to the general form $D_x=D_{m0}\cdot\exp(-E_m/kT)$ cm^2/s and $[X]^*=[X^0]^*\cdot\exp(-E_f/kT)$ cm^{-3}, respectively. The temperature dependence of deep levels and binding energies can be found in Ref. 12.

	V^{--}	V^-	V^0	V^+	V^{++}	I^-	I^0	I^+	AsV^-	AsV^0	AsV^+	As_i^0	As_i^+
$D_{m0}(\times10^{-3}$ cm^2/s)	1	1	1	1	1	5	5	5	0.21	0.21	0.21	4	4
E_m(eV)	0.4	0.4	0.4	0.6	0.8	1	1	1	1.6	1.3	1.3	1.4	1.4
$e_t-e_v(T=0)$(eV)	1.06	0.6		0.03	0.13	1		0.4	0.77		0.3		0.1
$[X^0]^*(\times10^{25}$ cm$^{-3})$			8.5				529						
E_f(eV)			3.8				3.8						
$E_b(T=0)$(eV)									1.6	1.3	1.01	1	0.1

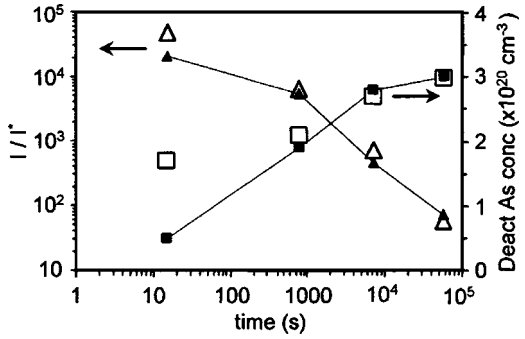

FIG. 3. Experimental (filled symbols) and simulated (open symbols) time evolution of I supersaturation (triangles) and electrically deactivated As concentration (squares), corresponding to the experiment shown in Fig. 2.

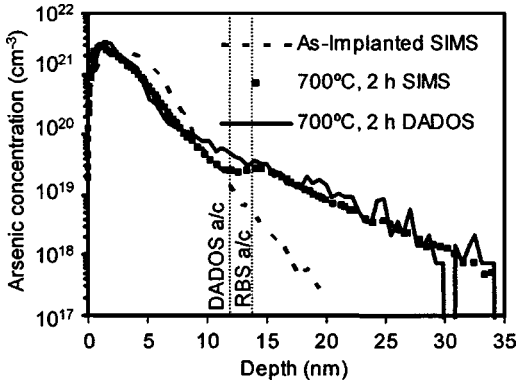

FIG. 4. SIMS data from Ref. 20 (symbols) and simulation (solid line) of 2 keV, 10^{15} cm^{-2} As profiles implanted into preamorphized Si (5 keV, 10^{15} cm^{-2} Ge) and annealed at 700 °C for 2 h. Notice that the simulated a/c interface is located at 12 nm from the surface, in good agreement with measurements (15 nm).

ing AsV that diffuse and combine with substitutional As forming As_2V, as it is shown in Fig. 1 (dotted arrow). After this step, the deactivation follows the same path explained before, being assisted by the mobile As_i.

Taking into account that the electrical solubility of As at the experiment temperature 1×10^{20} cm^{-3} (1), it can be seen that after 16 h annealing the As deactivation has not finished yet and that would go on at a much slower rate. Finally, notice that the simulation overestimates the deactivated As concentration for the first 15 s of the annealing (Fig 3). In fact, in our simulations, the formation of the clusters As_n is assumed to be instantaneous while in the experiments seems to be a thermally activated process with a very low activation energy. Therefore, this simplifying assumption is expected to be satisfactory for long term annealings but leads to an overestimation of the deactivate fraction for rapid thermal ones.

Finally, we also test the model with a representative As implant/annealing cycle applicable to the advanced sub-65 nm CMOS technology. The simulation of this experiment demands a correct modeling not only of the As kinetics but also of the rest of phenomena like damage buildup and amorphization, recrystallization[9] and extended defect ({311} defects, dislocation loops, and voids) nucleation and evolution. In the experiment,[20] the silicon wafer was preamorphized with 5 keV, 10^{15} cm^{-2} Ge implant followed by 2 keV, 10^{15} cm^{-2} As implant. Subsequently, the sample was annealed at 700 °C for 2 h to regrow the *a*-Si layer and to activate the As profile. In Fig. 4 both, experimental and simulated As profiles appear and the a/c interface position after Ge implantation. The initial point defect and arsenic profiles were calculated using the binary collision approximation. As can be clearly seen, the simulation properly reproduce the amorphous layer extension as well as the As profile after annealing. The amorphous layer created by the Ge implant is rapidly recrystallized during the temperature ramp-up and a fraction of the As atoms are swept towards the surface according to the As SPER segregation rate, producing the increase of the arsenic peak concentration in the regrown region. The simulation also suggests that the As transient enhanced diffusion is due to the excess of As_i generated by the end-of-range extended defects dissolution.

In summary, a comprehensive physical As model has been developed to explain As high concentration effects in silicon. With such a model As rapid electrical deactivation can be fairly reproduced and it can be also extended to preamorphized high As concentration implants.

This work has been partially supported by the Spanish Government under Project No. BFM2001-2250 and by the Castilla y Leon regional Government under Project No. VA-010/02.

[1] D. Nobili, S. Solmi, A. Parisini, M. Derdour, A. Armigliato, and L Moro, Phys. Rev. B **49**, 2477 (1994).
[2] S. Solmi, D. Nobili, and J. Shao, J. Appl. Phys. **87**, 658 (2000).
[3] M. Ramamoorthy and S. T. Pantelides, Phys. Rev. Lett. **76**, 4753 (1996).
[4] D. C. Mueller, E. Alonso, and W. Fichtner, Phys. Rev. B **68**, 045208 (2003).
[5] K. C. Pandey, A. Erbil, G. S. Cargill, and R. F. Boehme, Phys. Rev. Lett. **61**, 1282 (1988).
[6] V. Ranki, J. Nissilä, and K. Saarinen, Phys. Rev. Lett. **88**, 105506 (2002).
[7] D. W. Lawther, U. Myler, P. J. Simpson, P. M. Rousseau, P. B. Griffin, and J. D. Plummer Appl. Phys. Lett. **67**, 3575 (1995).
[8] M. Jaraiz, P. Castrillo, R. Pinacho, I. Martin-Bragado, and J. Barbolla, in *Simulation of Semiconductor Processes and Devices 2001 (SISPAD'01)*, edited by D. Tsoukalas and C. Tsamis (Springer, Vienna, 2001), p. 10.
[9] J. E. Rubio, M. Jaraiz, I. Martin-Bragado, R. Pinacho, P. Castrillo, and J. Barbolla, Mater. Sci. Eng., B **114-115**, 151 (2004).
[10] N. E. B. Cowern, G. Mannino, P. A. Stolk, F. Roozeboom, H. G. A. Huizing, J. G. M van Berkum, F. Cristiano, A. Claverie, and M. Jaraiz, Phys. Rev. Lett. **82**, 4460 (1999)
[11] P. M. Fahey, P. B. Griffin, and J. D. Plummer, Rev. Mod. Phys. **61**, 289 (1989).
[12] I. Martin-Bragado, R. Pinacho, P. Castrillo, M. Jaraiz, J. E. Rubio, and J. Barbolla, Mater. Sci. Eng., B **114–115**, 284 (2004).
[13] *Taurus Reference Manual, version 2002.2*, Avanti Corp., Fremont, USA.
[14] S. Matsumoto, Y. Ishikawa, and T. Niimi, J. Appl. Phys. **54**, 5049 (1983)
[15] R. B. Fair, in *Impurity Doping*, edited by F. F. Y. Wang (North-Holland, Amsterdam, 1981), Chap. 7, p. 315.
[16] P. M. Rousseau, P. B. Griffin, and J. D. Plummer, Appl. Phys. Lett. **65**, 578 (1994).
[17] P. M. Rousseau, P. B. Griffin, W. T. Fang, and J. D. Plummer, J. Appl. Phys. **84**, 3593 (1998).
[18] P. M. Rousseau, P. B. Griffin, S. C. Kuehne, and J. D. Plummer, IEEE Trans. Electron Devices **43**, 547 (1996).
[19] S. Solmi, M. Ferri, M. Bersani, D. Giubertoni, and V. Soncini, J. Appl. Phys. **94**, 4950 (2003).
[20] V. C. Venezia, R. Duffy, L. Pelaz, M. Aboy, A. Jeringa, P. B. Griffin, C. C. Wang, M. J. P. Hopstaken, Y. Tamminga, T. Dao, B. J. Pawlak, and F. Roozeboom, IEDM 2003.